Proceedings of the ASME 2023
International Mechanical Engineering Congress and Exposition
IMECE2023
October 29-November 2, 2023, New Orleans, Louisiana

IMECE2023- 112025

CONDITION MONITORING OF CUTTING TOOLS BY FEATURE ANALYSIS OF VIBRO-ACOUSTIC SENSING SIGNALS

Dongjing Lao
University of Michigan-Shanghai Jiao Tong
University Joint Institute, Shanghai Jiao Tong
University, Shanghai, China

Yanfeng Shen
University of Michigan-Shanghai Jiao Tong
University Joint Institute, Shanghai Jiao Tong
University, Shanghai, China

ABSTRACT

This paper presents a vibro-acoustic sensing method for real-time Tool Condition Monitoring (TCM) for Computerized Numerical Control (CNC) machining. The method captures Contact Acoustic Nonlinearity (CAN) arising from periodic impacts between the cutting teeth and the workpiece to obtain the spectral domain characteristics of sensing signals captured by piezoelectric transducers. The tool wear evaluation metric is constructed, starting with analytical modeling of cutting signals using a nonlinear oscillator model. Numerical case studies are conducted where a periodic impact vibration signal is simulated and fed into the equivalent CAN reduced-order nonlinear oscillator model of a machine tool system to predict the dynamic response. Thus, the nonlinear response spectrum is obtained and the mechanism behind the spectral nonlinear characteristics is illustrated by simulating various wear severities and breakage situations of the cutting tool. Furthermore, nonlinear features are extracted from the vibration response acquired during CNC machine tool machining by low-cost piezoelectric sensors to diagnose the tool damage. Several damage indices are explored to quantify the severity of the damage, relating to spectral nonlinear features such as shifts in the position of the dominant frequency, increase in mixed-frequency response components, and generation of higher-order harmonic components. The analytical modeling results, the extracted non-linear features, and the damage index derived is validated against experiments and are able to effectively identify the severity of tool wears. The proposed method and findings provide a promising approach for the practical application in the field of smart manufacturing.

Keywords: tool condition monitoring, vibro-acoustics, smart manufacturing, wearing and tipping detection, nonlinear feature

1. INTRODUCTION

A new era of industry characterized by enhanced efficiency, profitability, and sustainability has been ushered in by the advent of intelligent manufacturing [1]. Within this framework, the utilization of Computerized Numerical Control (CNC) machinery, equipped with novel sensing technology, has emerged as a pivotal strategy for the real-time assessment of machining reliability [2, 3]. It should be noted that certain scenarios, such as intermittent cutting, high-speed operations, and heavy loads, can result in abrupt tool failure due to extreme mechanical stress, thermal stress, or shocks. Serious effects on machining quality and efficiency, as well as unplanned downtime leading to economic loss and life safety issues, can result from unpredicted wearing, cracking, and tipping of cutting tools [4]. Consequently, the development and implementation of Tool Condition Monitoring (TCM) techniques assume paramount significance in averting catastrophic incidents during machining operations.

TCM has emerged as a prominent area of research in industry, showcasing a well-established system architecture as a result of advancements in sensing technology and artificial intelligence [5, 6]. Notably, the primary focus of TCM investigations has centered on the monitoring of tool wear, encompassing the recognition of wear states, monitoring the width of flank wear (VB), and predicting the Remaining Useful Life (RUL). Two mainstream approaches have been employed in TCM: direct monitoring and indirect monitoring. The direct monitoring method relies on machine vision, which presents challenges in effectively detecting sudden tool breakage during machining operations. Furthermore, it is susceptible to the influences of cutting fluids, lighting conditions, and chip interference, necessitating interruptions for measurement purposes. Conversely, indirect monitoring methods in TCM, employing data-driven approaches and embedded sensors within manufacturing systems, offer cost-effective and practical solutions for industrial applications. During the cutting process, a significant amount of systematic feedback on tool conditions is generated. Physical signals for data analysis can be collected by different sensors, such as cutting force [7–9], Acoustic Emission (AE) [10–12], vibration [13, 14], sound [15], spindle motor power [16] and currents [17]. The selection of appropriate sensors holds paramount importance in ensuring signal quality and facilitating the characterization of tool conditions.

Vibro-acoustic sensing methods were employed to acquire vibration signals from machine tools, thereby presenting a cost-effective and easily installable approach for monitoring tool conditions. The vibration signal contains various components providing valuable insights into tool condition, such as the friction between the tool and workpiece, machine vibration, and tool cut-in/cut-out. In a study conducted by W. Rmili et al. in 2016 [18], vibration characteristics, including mean, effective and peak-to-peak values, showed an increasing trend as flank wear progressed, identifying three different stages of tool wear based on statistical analysis methods. Nevertheless, the recognition of these signatures is prone to errors due to the vibration signal's low signal-to-noise ratio. Hence, there is a need to investigate feature values that are less susceptible to noise for the purpose of determining tool conditions.

The stability and non-linearity of the tooling are determined by the integration of multiple structural components within the machine. It is noteworthy that the vibration feedback signal of the system, obtained from a periodic vibration signal source, displays a nonlinear response that effectively represents the nonlinear characteristics associated with the system's condition and is less vulnerable to disturbances from the environment. Consequently, the exploration of these nonlinear characteristics holds the potential to enhance the accuracy of diagnosing tool wear.

This paper presents a vibro-acoustic sensing method for real-time monitoring of wearing, cracking, and tipping of cutting tools. The current research initiates by formulating an analytical model using a nonlinear oscillator model to capture the Contact Acoustic Nonlinear (CAN) response [19]. Subsequently, numerical simulations were conducted to study various levels of tool wear and breakage, including the wear of tools with different numbers of cutting teeth and different wear influence parameters. The purpose of these simulations was to illustrate the underlying mechanisms of the nonlinear features observed in the spectral response, such as the superharmonic and shock vibrations that contribute to the mixed frequency response. Additionally, nonlinear features were extracted from the vibration acoustic response signals obtained during machining on machines, using a low-cost, flexible Piezoelectric Wafer Active Sensor (PWAS). Damage indices were developed to quantify the severity of damage, and the results were experimentally verified to be effective in identifying the severity of tool wear.

2. SIMULATION OF CUTTING RESPONSE

For the overall system of the machine tool, the cutting response corresponds to the feedback of the impact signal generated by the tool's attack on the workpiece. As depicted in Figure 1, the initiation of a cutting cycle occurs when the workpiece is instantaneously impacted by the tool, leading to the creation of a cutting layer, which is subsequently followed by the gradual shedding of chips. The workpiece is cut into by the tools, creating bonding and mutual vibration. The vibration damping decays due to the influence of the friction forces F_{ff} and F_{fa} generated between the tool, the workpiece, and the chip, in addition to the material damping of the workpiece. The amplitude of the impact vibration is controlled by the cutting force Fc. Periodic amplitude modulation of the vibration signal can be induced by unevenness in the magnitude of the cutting force caused by tool wear. [20].

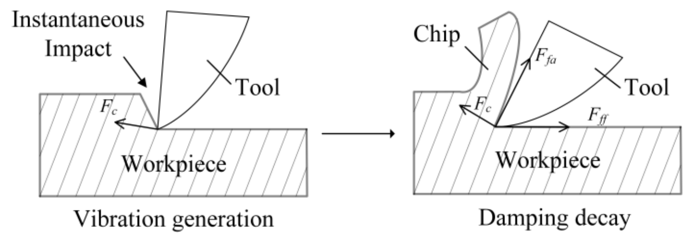

FIGURE 1: TOOL CUTTING PROCESS DIAGRAM

Based on the above tool cutting process, the simulation signals are used for modelling the impact signal generation cycle tool cutting [21, 22]. The simulation signal representing the unit cutting force of the tool is expressed by the following by Eq. (1).

$$\begin{cases} x(t) = s(t) + n(t) = \sum_i A_i h(t - iT) + n(t) \\ h(t) = \exp(-Ct)\cos(2\pi f_n t) \\ A_i = 1 + A_0 \cos(2\pi f_r t) \end{cases} \tag{1}$$

where $x(t)$ denotes the observed signal, s(t) emulates the periodic impact component of a four-tooth tool, and $n(t)$ represents the Gaussian noise signal, with the case studies being the theoretical input signal with a value of 0. The amplitude modulation A_0 is contingent upon the irregularities in the wear, and the rotation frequency f_r is specified as 50 Hz (3000r/min). Additionally, the attenuation coefficient C is set to 700, and the resonance frequency f_n is established at 8 kHz which is associated with the properties of both the tool and the workpiece. It is crucial to note that the eigenfrequency of the single tooth failure, denoted as f_{eig}, amounts to 200 Hz, thus establishing the impact period T at 5 ms.

As demonstrated in Figure 2(a)(b), the temporal waveform and spectrum of the simulation signal were obtained when the unit cutting force was multiplied by 20, with A_0 set to 0.02. The sampling frequency was 10 MHz and the signal length spanned 2 M data points. It is worth noting that the tool's interaction with the workpiece transpires at a consistent rate of every 5 ms, aligning with the frequency of the impact peaks evident in the simulated temporal signal. Upon analyzing the spectrum of the simulation signal, it becomes evident that distinct frequency components appear at intervals of 200 Hz, which correspond to the eigenfrequency associated with tool failure.

CAN is a manifestation of the intricate nonlinearity inherent in the machine tool, which arises from the functioning of diverse internal structural components and the frictional interaction [23]. The dynamic behavior of contact at interfaces undergoing periodic collisions leads to alterations in local structural stiffness. Moreover, the total stiffness of the machine tool's working system is significantly influenced by components such as screw nuts, guide slides, supporting angular contact ball bearings (ACBBs), and leadscrews. To simplify the representation of the nonlinear machine tool model and incorporate the characteristics of CAN resulting from the periodic cutting of each tooth on the workpiece, a reduced-order nonlinear oscillator model is employed to simulate the tool cutting process.

Figure 2(c)(d) presents the dynamic response that was obtained by feeding the impact signal into the nonlinear system. To simulate the practical signal acquisition process, such a response signal was extracted from the response of the 10M sampling rate to the signal component of 50K sampling rate, mimicking a practical data acquisition device capability.

The spectra comparisons between the input cutting signal and the response signal in Figure 2(b)(d) exhibit striking distinctions. The response signal from the nonlinear system demonstrates noticeable morphological changes and shifts in position, with a prominent concentration of frequencies both around 6 kHz and in the low-frequency region. Notably, at the integer multiple failure eigenfrequency 200n Hz, the response exhibits higher energy accumulation when compared to the simulated cutting signal. Furthermore, an interesting trend is observed in the 0 - 1 kHz interval, where the amplitude of frequency components transitions from gradual increments to gradual decrements. Common nonlinear features such as superharmonics are also observed in the vibration response signal, and yet their amplitude is so small that would be masked by noise.

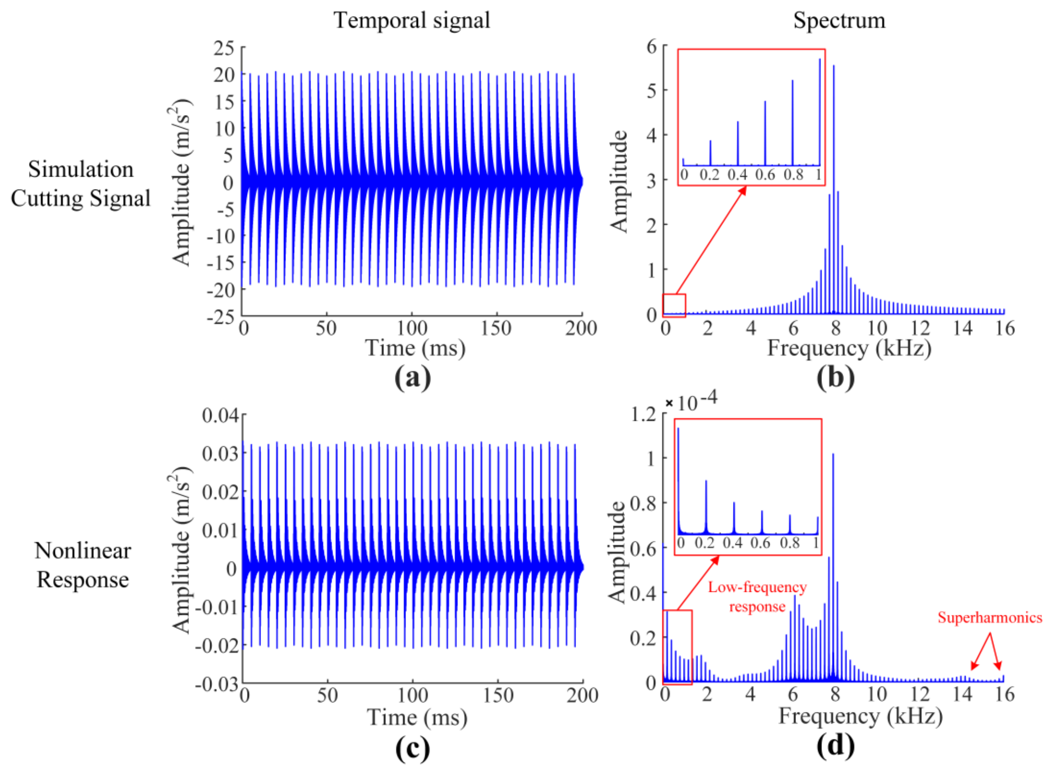

FIGURE 2: THE SIMULATED CUTTING SIGNAL: (A) TEMPORAL CUTTING SIGNAL; (B) CUTTING SIGNAL SPECTRUM; (C) THE NONLINEAR OSCILLATOR TEMPORAL SIGNAL; (D) SPECTRUM OF THE NONLINEAR RESPONSE

3. RESPONSE CHARACTERISTICS FOR VARIOUS TOOL WEARING SEVERITIES

In this section, several numerical case studies are analyzed by evaluating the impact of different levels of tool wear types on the system. The characteristics of the nonlinear response signal were explored by varying the system input signal with different wear conditions.

3.1 Modeling of progressive tool wear conditions

Intuitively, it can be observed that the Depth of Cut (DOC) is decreased as the length of each tooth of the tool is gradually worn down in Figure 3. The reduction of DOC exerts an influence on both the single-tooth amplitude A_i and amplitude modulation A_0 of the simulated impact signal in Eq. (1). The decrease in DOC is associated with a reduction in the cutting force experienced by an individual tooth, coupled with an increase in the unevenness of impacts among the teeth. As a consequence, A_i experiences a decrement, while A_0 undergoes an increment. The wear coefficient, as utilized in this research, serves to indicate the relative reduction of DOC from its initial state under practical working conditions.

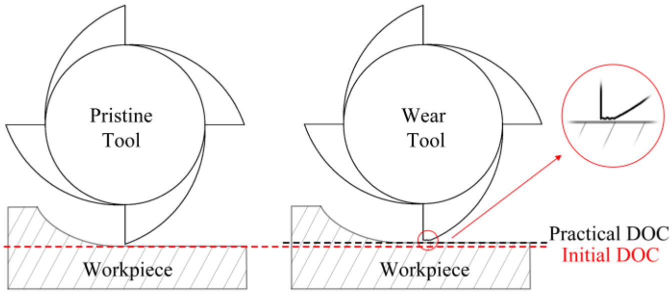

FIGURE 3: DEPTH OF CUT REDUCTION DIAGRAM

In addition, the variation in system stiffness and damping during the cutting process has been attributed to the interaction between the tool and the workpiece in recent studies [24, 25]. As the tool gradually wears down and the temperature rises, leading to intensified friction between the tool and workpiece, noticeable alterations in the tool shape and the appearance of micro-cracks were observed. These modifications would subsequently cause an increase in system nonlinearity and a decrease in resonant frequency due to the additional stiffness and damping induced.

Given the highly non-linear nature of the machine tool system, the small non-linear increments resulting from tool wear are considered negligible, and only significant changes to the input signal are taken into account in this research.

3.2 Tool wear response analysis

The impact cutting signals of the machine tool system are directly affected by the condition of tool wear, which results in changes in the vibration response signals. The wear signal is obtained from the initial simulation signal using the periodical tukey window for the purpose of reducing the cutting force on a single tooth. The wear tooth impact signal is shown in Figure 4(a) which the wear coefficient is gradually increased from 0% to 50%.

Figure 4(b) displays the impact temporal signal of a single tooth with a 50% wear coefficient. It is assumed that the other three teeth ideally maintain the initial cutting force. The peak envelope of the signal, highlighted in red, appears to be the outcome of multiple low-period sinusoidal waveforms superimposed on one another. Figure 4(c) illustrates the wear spectra where, as expected, frequency components below the eigenfrequency become evident. Additionally, the wear response spectrum in Figure 4(d) exhibits more pronounced frequency clustering at 50 Hz, 100 Hz, and 150 Hz. Regarding the eigenfrequency component, it is observed that there is a gradual decrease, which, when compared to the low-frequency component, does not show significant changes.

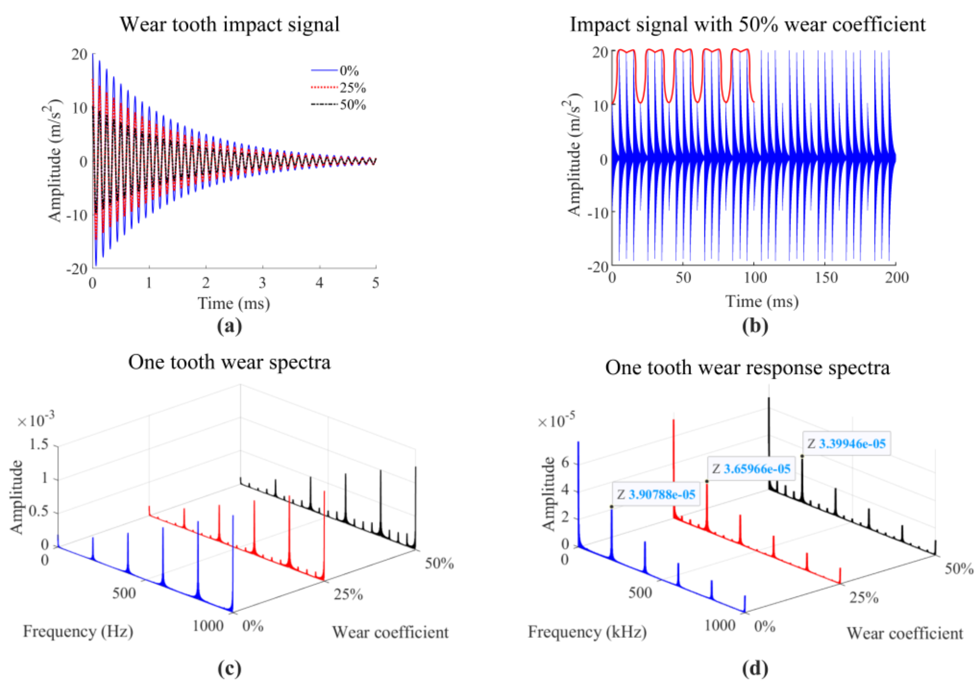

FIGURE 4: ANALYSIS FOR ONE-TOOTH WEAR CASE: (A) IMPACT SIGNALS WITH DIFFERENT WEAR COEFFICIENTS; (B) IMPACT TEMPORAL SIGNAL WITH A 50% WEAR COEFFICIENT; (C) SPECTRA OF CUTTING FORCE SIGNALS; (D) SPECTRA OF RESPONSE SIGNALS

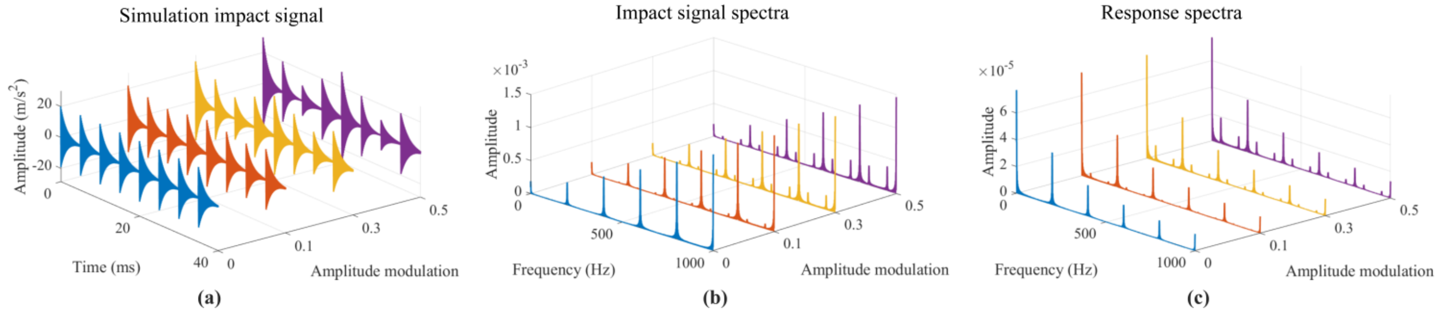

FIGURE 5: ANALYSIS OF AMPLITUDE MODULATION WITH 0% WEAR COEFFICIENT: (A) SIMULATED IMPACT SIGNAL; (B) SPECTRA OF CUTTING FORCE SIGNALS; (C) SPECTRA OF RESPONSE SIGNALS

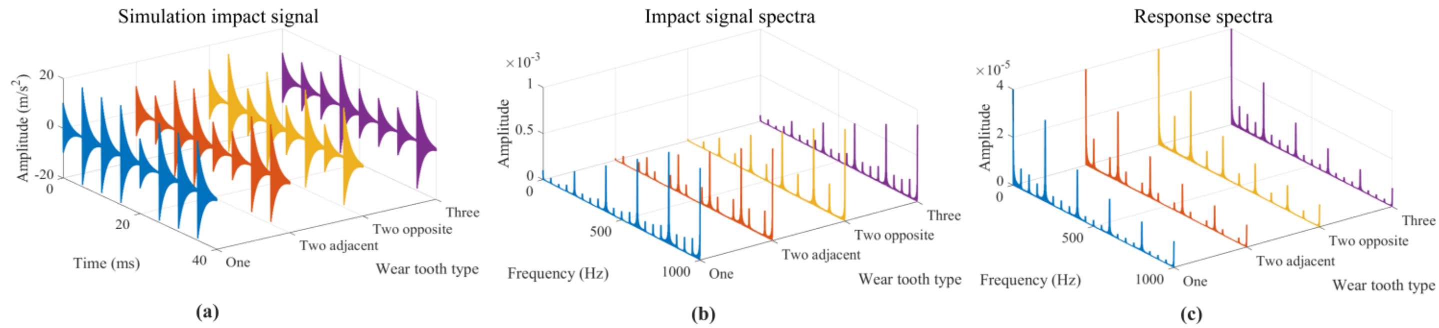

FIGURE 6: ANALYSIS OF WEAR TOOTH TYPES WITH 50% WEAR COEFFICIENT: (A) SIMULATED IMPACT SIGNAL; (B) SPECTRA OF CUTTING FORCE SIGNALS; (C) SPECTRA OF RESPONSE SIGNALS

With the progression of tooth wear, the tool generates tangential vibrations attributed to the disparity in cutting force magnitude. Consequently, the impact of increased amplitude modulation on the cutting signal is considered. Nevertheless, the amplitude modulation of the tool causes the cutting forces to oscillate cyclically, which again exacerbates the unevenness of the cutting forces. The effect of amplitude modulation on the impact signal with 0% wear coefficient is presented in Figure 5. This positive feedback process significantly reduces machining safety. It can be clearly seen from Fig. 5(b)(c) that the new frequency increases gradually around the eigenfrequency, i.e $200n \pm 50$ Hz. The reason for these phenomena is that amplitude modulation mainly causes the tool to oscillate periodically at the rotation frequency f_r in the theoretical model from Eq. (1). In reality the oscillation period of the tool is related to factors such as rotational speed, cutting forces and workpiece characteristics et al., which is a very complex issue. In summary, the effect of amplitude modulation is to produce new frequency components $nf_{eig} \pm f_{ri}$.

Additionally, the number and location of the worn teeth are taken into account, with the teeth being divided into one tooth, two adjacent teeth, two opposite teeth, three teeth. The impact signal and nonlinear response spectra for the simulation of four types of worn teeth are shown in Figure 6. The wear of different teeth produces low frequency components, but in different patterns, mainly concentrated at 50 Hz, 100 Hz, and 150 Hz. The root cause is the same as the one-tooth wear analysis above. The reduction in cutting force caused by the worn tooth causes the impact signal to be depressed, with the depression occurring at a frequency lower than the eigenfrequency and integer multiples of the rotational frequency.

Comprehensively, the above case study shows that the CAN vibration signal characteristics of the machine tool are mainly concentrated in the low-frequency band. The reduction of the depth of cut due to tool wear, and thus the cutback and non-uniformity of the cutting force are the main reasons for the differentiation of the nonlinear response spectrum. It is worth noting that the main features in the spectrum were analyzed in the theoretical model to be related to the rotation frequency f_r and the eigenfrequency f_{eig}, but the actual machining tool may have additional frequency components due to slip and tangential vibration. In order to clarify the effect of the independent variables on the nonlinear response spectrum, quantitative criteria must be established.

3.3 Quantification of the tool wear severity

The process of tool wear is known to be progressively unstable, and it is essential for the TCM system to possess the capability to detect and quantify the distinctions in the nonlinear response spectrum that arise as a result of tool wear. As tool wear can cause more sensitive feature changes in the low-frequency region of the nonlinear response signal, the quantitative metrics mainly is mainly used below1 kHz.

A tool wear metric is introduced in this section to carry out the quantitative analysis of tool wear condition, which is the

Root Mean Square Deviation (RMSD). The mathematical formula for the index is expressed as follows:

$$\mathrm{RMSD} = \sqrt{\int (A(f) - A_0(f))^2 df \,/\, \int A_0^2(f) df} \tag{2}$$

where $A(f)$ is the amplitude of nonlinear response spectrums. A_0 is the baseline spectrum shown in Figure 2(d).

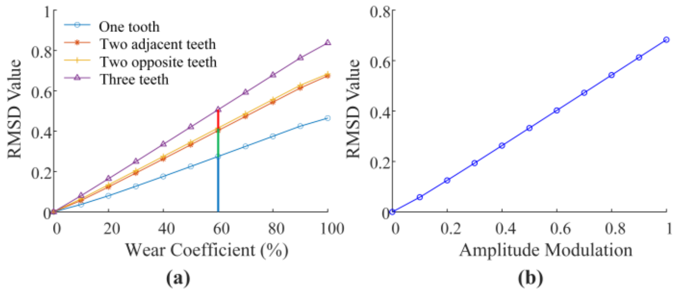

FIGURE 7: RMSD APPLIED TO EACH TOOL WEAR CASE STUDY: (A) VARIOUS WEAR TOOTH TYPES; (B) VARIOUS AMPLITUDE MODULATIONS

The evaluation of the severity of tool wear is accomplished by quantifying the difference in the nonlinear response spectrum using the tool wear index. This index takes into account various factors such as the shift of eigenfrequency and changes in amplitude, trends in low-frequency components, and the appearance of uncertain new peaks. By considering these factors, the tool wear index serves as a dependable tool for assessing the conditions of tool wear in different cases. RMSD was applied to each tool wear variable case study and the trends were summarized in Figure 7. It can be clearly seen that the EMSD values show an almost linear positive correlation with the wear coefficients in different cases. Interestingly, with an increase in the number of teeth worn, the RMSD also increases, but the increments become progressively smaller. The specific explanation is shown by the marked line in Figure 7(a), where the increment of RMSD for one-tooth wear is almost equal to half of the increment of RMSD for three-tooth wear. The increment of RMSD value decreases gradually from one-tooth to two-tooth to three-tooth wear. As a result, the first tooth worn will have a particularly significant increase in the RMSD value. Similarly, as depicted in Figure 7(b), the effect of amplitude modulation on the increase of RMSD is linearly positively correlated.

However, in real operating conditions, the wear coefficient shows a complex relationship with amplitude modulation. For example, tangential vibration of the tool is exacerbated by differences in the location and extent of tool wear, while conversely, increased damping due to the attachment of additional material to the front of the tool or insufficient lubrication may reduce the degree of amplitude modulation. All of these reasons may lead to irregular fluctuations in the RMSD value.

From the above analysis, it is emphasized that this indicator has a high sensitivity to the initial wear of the tool and can be analyzed effectively.

4. EXPERIMENTAL RESULTS AND DISCUSSION

In this section, the feasibility of RMSD wear metric is verified by performing tool wear tests on a machine tool experimental setup.

4.1 Vibro-acoustic sensing experimental setup

The experimental setup illustrated in Figure 8 comprises a manual drilling machine tool and acquisition apparatus. A four-tooth tool made of high-strength 3D printed material was employed for manual wear testing in the study. With each successive machining of a workpiece, the severity of tool wear gradually increases, resulting in an erratic growth in the amount of tool wear as the number of machining cycles progresses. A flexible PWAS receiver was fixed above the machine spindle to accommodate irregular surfaces and capture vibration signals pertaining to tool wear condition effectively. The tool's impact vibration signal was produced by its downward spindle feed and cutting against the workpiece. The receiver PWAS converted the machine tool's nonlinear response vibration into an analog electrical signal. The receiver PWAS was connected to the NI acquisition card by a coaxial line to minimize environmental interference and improve signal-to-noise ratio. The rotation speed of the drilling machine was selected as 3000 r/min, that mean the eigenfrequency is equal to the simulation model. The acquisition card recorded nonlinear response vibration signals of the system, which contained information about the tool wear condition, at a sampling rate of 50 kHz. Each acquisition lasted for 5 seconds.

FIGURE 8: EXPERIMENTAL SETUP

4.2 Tool wear metric validation

In this study, the test investigations consisted of 20 groups obtained from 20 consecutive machining operations on the same experimental four-tooth tool, which eventually wore out to the point where the tool became unusable. The pristine tool's nonlinear response signal served as the baseline for assessing the influence of the tool wear metric.

The signal obtained from the first machining was recorded as the baseline signal. The spectrum of the baseline signal is illustrated in Figure 9. A temporal signal of 200 ms duration presented in Figure 9(a) was intercepted from the complete acquired signal. In comparison to the simulated response signals in Figure 2(d), the experimental machine vibration spectrum displayed in Figure 9(b) exhibits a high degree of similarity, aligning well with the theoretical model. Likewise, at integer multiples of the eigenfrequency, distinct frequency components are observed, and their values gradually diminish, further validating the accuracy of the theoretical predictions in practical experimental settings. Due to the initial tool asymmetry and machining errors, many spurious peaks have appeared in the nonlinear vibration response spectrum, but in agreement with the theory there are frequency components appearing at 50 Hz, 100 Hz, and 150 Hz.

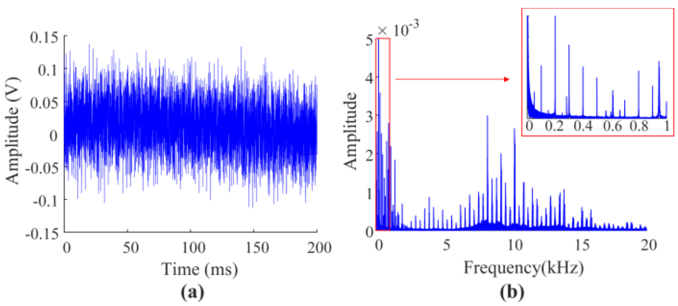

FIGURE 9: THE BASELINE SIGNAL: (A) TEMPORAL SIGNAL; (B) SPECTRUM

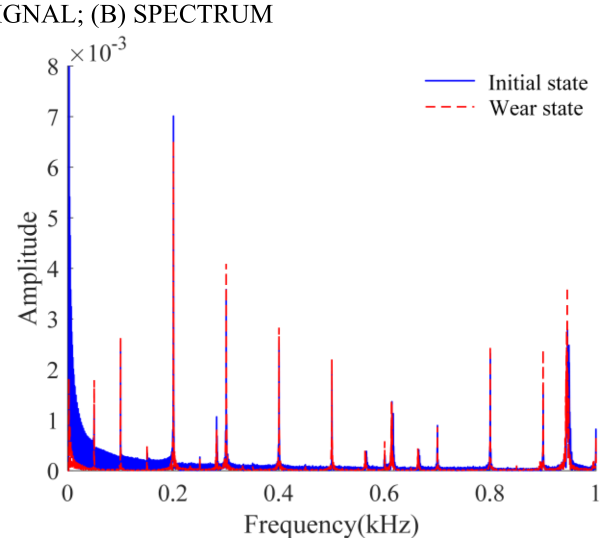

FIGURE 10: VIBRATION SPECTRUM OF TOOL WEAR STATE VS. INITIAL STATE

The spectrum of the cutting signal after tool wear is extracted and compared with the initial state, as shown in Figure 10. Particularly noteworthy were the significant decrease observed in the eigenfrequency, along with an increase in the content at other low-frequency components, such as 50 Hz, 150 Hz, 300 Hz, and beyond. Additionally, peak shifts were observed, as exemplified by the shift at 950 Hz. All of the mentioned changes in the features of the spectrum are attributed to tool wear.

In order to increase the accuracy of tool wear identification and to retain the necessary frequency components, such as the rotational frequency 50 Hz, very low frequency interference due to macro-irregular vibrations of the machine was filtered out. The RMSD metric was applied from 20 Hz to 1000 Hz and the RMSD trend graph is visualized in Figure 11. The horizontal coordinate indicates the number of machining cycles and also represents the severity of tool wear.

In the early stages of wear, the RMSD performed extremely sensitively, with a rapid increase in value of about 0.6. The sudden unexpectable tiny chipping of the tool resulted in large uneven cutting forces and generated amplitude modulation. The middle stage of tool wear was after the first wear tooth has appeared on the tool. Machining stability becomes less stable due to irregular tool vibrations and cutting force variations. RMSD values fluctuated within a range interval. As the number of machining cycles increases, high temperatures and frequent impacts degrade tool performance. Tool damage occurs uncontrollably and rapidly, entering the late stages of tool wear. The RMSD values gradually increased and even exceeded 1.

To recapitulate, the RMSD trend overall shows a consistent increase. The high sensitivity of RMSD to early tool wear was verified. Due to the material of the experimental tool, a high-strength metal tool under practical processing conditions was able to identify the early wear trend effectively. For severe tool wear RMSD still has some potential for sensing. Late wear of tools can be evaluated by setting thresholds and fluctuating standard deviations, etc.

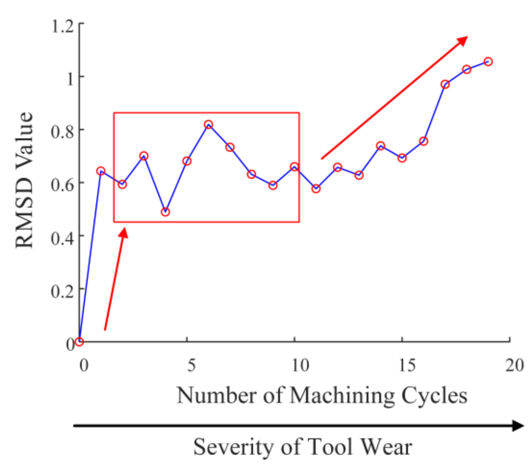

FIGURE 11: RMSD APPLIED TO DRILLING MACHINE MACHINING EXPERIMENT

5. CONCLUDING REMARKS

The current study presented a novel vibro-acoustic sensing approach for the real-time monitoring of the wearing, cracking, and tipping of cutting tools. Simulated machining signals are analyzed, and the corresponding contact acoustic nonlinearity response spectra are obtained for various influencing factors of the tool damage state. Based on the non-linear response spectrum, an RMSD metric was investigated for the characterization and evaluation of tool damage. Finally, the feasibility of the indicators was verified through the utilization of the proposed vibroacoustic sensing method to obtain the actual tool cutting vibration response. It was found that the RMSD metric has a high sensitivity to early wear and can be effectively utilized to evaluate the tool usage condition. For future work, more effective and informative wear metrics can be put forward through in-depth investigation of the characteristics of the nonlinear response spectrum and be practically applied to the real-time tool monitoring system of CNC machine tools. The theoretical study of tool wear in the frequency domain in this paper provides a general guidance for the subsequent optimization of fusion and enhancement of tool damage state monitoring techniques. The proposed methodology and the conclusions drawn provide a promising approach for future practical applications in the field of smart manufacturing.

ACKNOWLEDGEMENTS

The support from the National Natural Science Foundation of China (contract numbers 51975357 and 51605284) is thankfully acknowledged; this research is also sponsored by the Shanghai Rising-star Program (contract number 21QA1405100).

REFERENCES

[1] A. Kusiak, “Smart manufacturing must embrace big data,” *Nature*, vol. 544, no. 7648, pp. 23–25, Apr. 2017, doi: 10.1038/544023a.

[2] Q. Butler, Y. Ziada, D. Stephenson, and S. Andrew Gadsden, “Condition Monitoring of Machine Tool Feed Drives: A Review,” *J. Manuf. Sci. Eng.*, vol. 144, no. 10, Jun. 2022, doi: 10.1115/1.4054516.

[3] P. Jia, Y. Rong, and Y. Huang, “Condition monitoring of the feed drive system of a machine tool based on long-term operational modal analysis,” *Int. J. Mach. Tools Manuf.*, vol. 146, p. 103454, Aug. 2019, doi: 10.1016/j.ijmachtools.2019.103454.

[4] J. Dou, S. Jiao, C. Xu, F. Luo, L. Tang, and X. Xu, “Unsupervised online prediction of tool wear values using force model coefficients in milling,” *Int. J. Adv. Manuf. Technol.*, vol. 109, Jul. 2020, doi: 10.1007/s00170-020-05684-1.

[5] T. Mohanraj, S. Shankar, R. Rajasekar, N. R. Sakthivel, and A. Pramanik, “Tool condition monitoring techniques in milling process — a review,” *J. Mater. Res. Technol.*, vol. 9, no. 1, pp. 1032–1042, Jan. 2020, doi: 10.1016/j.jmrt.2019.10.031.

[6] X. Li, X. Liu, C. Yue, S. Y. Liang, and L. Wang, “Systematic review on tool breakage monitoring techniques in machining operations,” *Int. J. Mach. Tools Manuf.*, vol. 176, p. 103882, May 2022, doi: 10.1016/j.ijmachtools.2022.103882.

[7] M. Jamshidi, X. Rimpault, M. Balazinski, and J.-F. Chatelain, “Fractal analysis implementation for tool wear monitoring based on cutting force signals during CFRP/titanium stack machining,” *Int. J. Adv. Manuf. Technol.*, vol. 106, no. 9–10, pp. 3859–3868, Feb. 2020, doi: 10.1007/s00170-019-04880-y.

[8] K. Zhu, T. Mei, and D. Ye, “Online Condition Monitoring in Micromilling: A Force Waveform Shape Analysis Approach,” *IEEE Trans. Ind. Electron.*, vol. 62, no. 6, pp. 3806–3813, Jun. 2015, doi: 10.1109/TIE.2015.2392713.

[9] G. Wang, Y. Yang, and Z. Li, “Force Sensor Based Tool Condition Monitoring Using a Heterogeneous Ensemble Learning Model,” *Sensors*, vol. 14, no. 11, pp. 21588–21602, Nov. 2014, doi: 10.3390/s141121588.

[10] M. S. H. Bhuiyan, I. A. Choudhury, M. Dahari, Y. Nukman, and S. Z. Dawal, “Application of acoustic emission sensor to investigate the frequency of tool wear and plastic deformation in tool condition monitoring,” *Measurement*, vol. 92, pp. 208–217, Oct. 2016, doi: 10.1016/j.measurement.2016.06.006.

[11] Q. Ren, L. Baron, M. Balazinski, R. Botez, and P. Bigras, “Tool wear assessment based on type-2 fuzzy uncertainty estimation on acoustic emission,” *Appl. Soft Comput.*, vol. 31, pp. 14–24, Jun. 2015, doi: 10.1016/j.asoc.2015.02.037.

[12] Q. Ren, M. Balazinski, L. Baron, K. Jemielniak, R. Botez, and S. Achiche, “Type-2 fuzzy tool condition monitoring system based on acoustic emission in micromilling,” *Inf. Sci.*, vol. 255, pp. 121–134, Jan. 2014, doi: 10.1016/j.ins.2013.06.010.

[13] Z. Lei, Q. Zhu, Y. Zhou, B. Sun, W. Sun, and X. Pan, “A GAPSO-Enhanced Extreme Learning Machine Method for Tool Wear Estimation in Milling Processes Based on Vibration Signals,” *Int. J. Precis. Eng. Manuf.-Green Technol.*, vol. 8, no. 3, pp. 745–759, May 2021, doi: 10.1007/s40684-021-00353-4.

[14] Y. Fu, Y. Zhang, H. Gao, T. Mao, H. Zhou, R. Sun, and D. Li, “Automatic feature constructing from vibration signals for machining state monitoring,” *J. Intell. Manuf.*, vol. 30, no. 3, pp. 995–1008, Mar. 2019, doi: 10.1007/s10845-017-1302-x.

[15] A. Kothuru, S. P. Nooka, and R. Liu, “Application of audible sound signals for tool wear monitoring using machine learning techniques in end milling,” *Int. J. Adv. Manuf. Technol.*, vol. 95, no. 9, pp. 3797–3808, Apr. 2018, doi: 10.1007/s00170-017-1460-1.

[16] M. Nouri, B. K. Fussell, B. L. Ziniti, and E. Linder, “Real-time tool wear monitoring in milling using a cutting condition independent method,” *Int. J. Mach. Tools Manuf.*, vol. 89, pp. 1–13, Feb. 2015, doi: 10.1016/j.ijmachtools.2014.10.011.

[17] Y. Zhou and W. Sun, “Tool Wear Condition Monitoring in Milling Process Based on Current Sensors,” *IEEE Access*,

vol. 8, pp. 95491–95502, 2020, doi: 10.1109/ACCESS.2020.2995586.

[18] W. Rmili, A. Ouahabi, R. Serra, and R. Leroy, "An automatic system based on vibratory analysis for cutting tool wear monitoring," *Measurement*, vol. 77, pp. 117–123, Jan. 2016, doi: 10.1016/j.measurement.2015.09.010.

[19] R. Lu, Y. Shen, B. Zhang, and W. Xu, "Nonlinear Electro-Mechanical Impedance Spectroscopy for fatigue crack monitoring," *Mech. Syst. Signal Process.*, vol. 184, p. 109749, Feb. 2023, doi: 10.1016/j.ymssp.2022.109749.

[20] R. B. Randall, J. Antoni, and S. Chobsaard, "THE RELATIONSHIP BETWEEN SPECTRAL CORRELATION AND ENVELOPE ANALYSIS IN THE DIAGNOSTICS OF BEARING FAULTS AND OTHER CYCLOSTATIONARY MACHINE SIGNALS," *Mech. Syst. Signal Process.*, vol. 15, no. 5, pp. 945–962, Sep. 2001, doi: 10.1006/mssp.2001.1415.

[21] Q. Wang, L. Wang, H. Yu, D. Wang, and A. K. Nandi, "Utilizing SVD and VMD for Denoising Non-Stationary Signals of Roller Bearings," *Sensors*, vol. 22, no. 1, 2022, doi: 10.3390/s22010195.

[22] J. Antoni, F. Bonnardot, A. Raad, and M. El Badaoui, "Cyclostationary modelling of rotating machine vibration signals," *Mech. Syst. Signal Process.*, vol. 18, no. 6, pp. 1285–1314, Nov. 2004, doi: 10.1016/S0888-3270(03)00088-8.

[23] H. Miao, C. Wang, C. Li, W. Song, X. Zhang, and M. Xu, "Nonlinear dynamic modeling and vibration analysis of whole machine tool," *Int. J. Mech. Sci.*, vol. 245, p. 108122, May 2023, doi: 10.1016/j.ijmecsci.2023.108122.

[24] A. Iglesias, L. Taner Tunç, O. Özsahin, O. Franco, J. Munoa, and E. Budak, "Alternative experimental methods for machine tool dynamics identification: A review," *Mech. Syst. Signal Process.*, vol. 170, p. 108837, May 2022, doi: 10.1016/j.ymssp.2022.108837.

[25] A. W. Nemetz, W. Daves, T. Klünsner, W. Ecker, T. Teppernegg, C. Czettl, and I. Krajinović, "FE temperature- and residual stress prediction in milling inserts and correlation with experimentally observed damage mechanisms," *J. Mater. Process. Technol.*, vol. 256, pp. 98–108, Jun. 2018, doi: 10.1016/j.jmatprotec.2018.01.039.